

# Helical Structures of Conjugate Polymers Created by Oxidative Polymerization Using Synthetic Lipid Assemblies as Templates

Tsukasa Hatano,<sup>[a]</sup> Ah-Hyun Bae,<sup>[a]</sup> Masayuki Takeuchi,<sup>[a]</sup> Norifumi Fujita,<sup>[a]</sup>  
Kenji Kaneko,<sup>[b]</sup> Hirotaka Ihara,<sup>[c]</sup> Makoto Takafuji,<sup>[c]</sup> and Seiji Shinkai\*<sup>[a]</sup>

**Abstract:** The morphology of conjugate polymers (such as poly(ethylenedioxythiophene), poly(pyrrole), and poly(aniline)) can be controlled in their polymerization processes, by applying the concept of the templating method to oxidative polymerization. As oxidative polymerization of these monomers produces cationic intermediates, the anionic assemblies can act as potential templates due to the mutual electrostatic attractive force. Oxidative polymer-

ization of ethylenedioxythiophene (EDOT), pyrrole, and aniline was carried out using helical superstructures of synthetic lipid assemblies as templates. Interestingly, we have found that oxidative polymerization of these monomers results in novel polymeric aggre-

gates, such as a helical-tape structure and an intertwined helical structure, and that both the right-handed and left-handed helical structures can be created by a change in the hydrophilic head groups. This is the first example of helical superstructures composed of conjugate polymers that have been designed utilizing a convenient templating method.

**Keywords:** conjugate polymers • helical structures • lipids • polymerization • template synthesis

## Introduction

Recently, oriented polymers and/or polymer nanostructures have attracted wide attention.<sup>[1]</sup> Of particular interest have been structures that consist of conjugate polymers because of their potential application as electrochemical switches, electric devices, sensors, and so forth.<sup>[2,3]</sup> Poly(ethylenedioxythiophene) (poly(EDOT)), poly(pyrrole), and poly(aniline) (poly(ANI)) are conjugate polymers easily obtained by electrochemical or chemical polymerization of the corresponding monomers. So far, several attempts have been made to construct oriented polymers and/or polymer nanostructures, for example, deposition of monomers in the ori-

ented environments such as LB membranes,<sup>[4]</sup> surfactant aggregates,<sup>[5,6]</sup> and liquid crystals,<sup>[7]</sup> among others.<sup>[8,9]</sup> It is known, however, that the prediction of the resultant superstructures and the fine-tuning of the molecular assemblies in these systems are nearly impossible and in fact these superstructures are created, in most cases, just by accident.

Recently, we and others have explored a new method to transcribe a variety of organic superstructures into inorganic materials by a sol-gel reaction of metal alkoxides ("templating sol-gel reaction"), by which one can control the morphology of inorganic compounds and create various new superstructural inorganic materials.<sup>[10-18]</sup> The driving force operating in this templating sol-gel reaction is considered to be electrostatic and/or hydrogen-bonding interactions between silica nanoparticles and organic assemblies acting as templates.<sup>[16]</sup> Thus, it occurred to us that the morphology of these conjugate polymers would also be controllable by applying the concept of the templating method to the electrochemical polymerization process; that is, as oxidative polymerization of these monomers produces cationic intermediates, the anionic assemblies should act as a potential template due to the mutual electrostatic attractive force. More recently, we found that anionic polymers and assemblies, such as DNA superstructures, [60]fullerene encapsulated in *p*-sulfonatocalix[8]arene, J aggregates of 5,10,15,20-tetrakis(4-sulfonatophenyl)porphyrin, and single-walled carbon nanotubes dispersed by sodium dodecyl sulfate (SDS) or DNA, act as templates that can be readily deposited on the

[a] Dr. T. Hatano, A.-H. Bae, Dr. M. Takeuchi, Dr. N. Fujita,  
Prof. Dr. S. Shinkai  
Department of Chemistry and Biochemistry  
Graduate School of Engineering  
Kyushu University, Fukuoka 812-8581 (Japan)  
Fax: (+81)092-642-3611  
E-mail: seijitcm@mbox.nc.kyushu-u.ac.jp

[b] Prof. Dr. K. Kaneko  
HVEM Laboratory, Kyushu University  
Fukuoka 812-8581 (Japan)

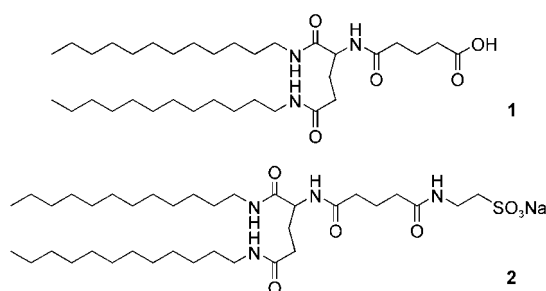
[c] Prof. Dr. H. Ihara, Dr. M. Takafuji  
Department of Materials and Life Science  
Graduate School of Science and Technology  
Kumamoto University, Kumamoto 860-8555 (Japan)

Supporting information for this article is available on the WWW under <http://www.chemeurj.org/> or from the author.

indium–tin oxide (ITO) electrode by electrochemical polymerization of these monomers.<sup>[19]</sup> Observation by scanning electron microscopy (SEM) established that the resulting conjugate-polymeric assemblies have superstructures similar to those of the original organic templates. These findings prompted us to apply this concept to some anionic organic templates bearing a helical superstructure. In this paper, we report that the helical superstructures are created from the assembly of conjugate polymers using chiral synthetic lipids as the templates.

## Results and Discussion

**Characterization of the morphology formed from anionic assemblies:** Superstructures of synthetic lipid molecules **1**<sup>[20]</sup> and **2**<sup>[21]</sup> were characterized by SEM and transmission electron microscopy (TEM) (Scheme 1).



Scheme 1. Structures of synthetic lipids **1** and **2** bearing an L-glutamic segment.

Figure 1a shows SEM and TEM images of aggregate **1** (obtained from an aqueous solution, [**1**] = 0.33 mM, NaOH = 2 mM). In both images, a fibrous structure with a right-handed helical motif was observed. In contrast, it was found that aggregate **2** (obtained from an aqueous solution, [**2**] = 0.3 mM, 10 vol% methanol) resulted in a fibrous structure with a left-handed helical motif (Figure 1b). These results imply that the helical motif of these synthetic lipids is inverted by the difference in the acidic head groups. In the aggregates prepared from **2**, a huge sheet structure (more than

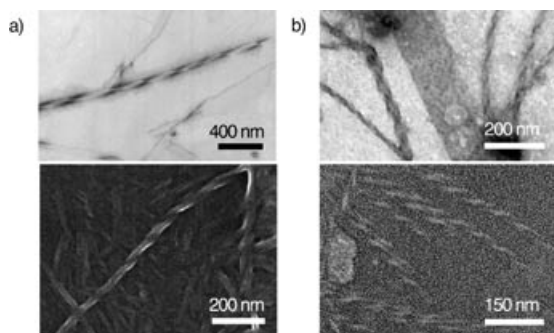


Figure 1. TEM (top) and SEM (bottom) images of lipid aggregates of a) **1** prepared from an aqueous solution containing 2 mM NaOH and b) **2** prepared from a 10 vol% MeOH aqueous solution. TEM analyses were performed after staining treatment with phosphotungstic acid.

200 nm in width) was observed in addition to the left-handed fibrous structure. This sheet structure also acts as a template to create novel intertwined polymeric aggregates by oxidative polymerization of ethylenedioxythiophene (see later).

**Electrochemical polymerization of EDOT, pyrrole, and aniline by a templating method:** Polymerization solutions containing EDOT and lipid aggregates were prepared as follows: a triethylene glycol solution (0.1 mL) containing EDOT (10 mg) was mixed with water (10 mL) under sonication. Compound **1** (2.0 mg), NaOH aqueous solution (1 M, 20  $\mu$ L), and LiCl (21 mg) were then added to this solution. Basic conditions were necessary to dissociate the proton of the carboxylic acid group to form the carboxylate group in **1**. In contrast, the sulfonate group in **2** can be dissociated under neutral conditions; that is, compound **2** (2.1 mg), EDOT (13 mg), and NaClO<sub>4</sub> (61 mg) were dissolved in a MeOH aqueous solution (10 vol%, 10 mL). The resultant solutions were used for subsequent electrochemical experiments. The cell consisted of an ITO electrode as the working electrode (working area = 2.2 cm<sup>2</sup>), a Pt counter electrode, and an Ag/AgCl reference electrode. In the electrochemical polymerization, the value of the electric current increased during the successive potential sweeping in the presence of **1** or **2** (Figure 2). The results indicate that the

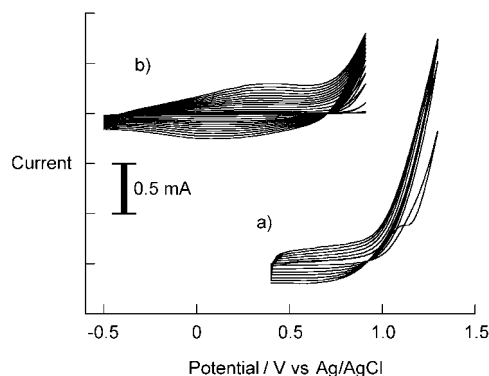


Figure 2. Cyclic voltammograms for EDOT obtained on an ITO electrode in the presence of a) **1** in an aqueous solution containing 2 mM NaOH (redox potential sweep between 0.4 and 1.3 V) and b) **2** in a 10 vol% MeOH aqueous solution (redox potential sweep between -0.5 and 0.9 V) at 25 °C.

poly(EDOT) films are deposited onto the ITO electrode. We found that to deposit the poly(EDOT) films, the redox potential range for electrochemical polymerization in the presence of **1** (0.4–1.3 V vs Ag/AgCl) should be more positive than that in the presence of **2** (-0.5–0.9 V vs Ag/AgCl). It is known that the electrochemical properties of poly(pyrrole) prepared in aqueous media (in particular, basic aqueous media) are inferior to those prepared in nonaqueous media due to side reactions of poly(pyrrole).<sup>[22]</sup> The presence of water, OH<sup>-</sup>, and/or Cl<sup>-</sup> ions in the polymerization solution has been suggested as the main reason for such side reactions.<sup>[23]</sup> Presumably, this is why the poly(EDOT) film in the presence of **1**, the formation of which is carried out

under basic conditions, requires the more severe redox conditions.

The oxidized and reduced states of the obtained poly(EDOT) films deposited onto the ITO electrode were characterized by UV-visible absorption spectroscopy (Figure 3).

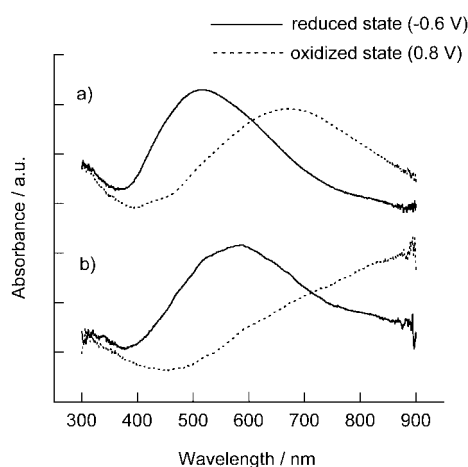


Figure 3. UV-visible absorption spectra of poly(EDOT) films in reduced (—) and oxidized (---) states electrodeposited onto an ITO electrode in the presence of a) **1** in a 50 mM LiCl aqueous solution and b) **2** in a 50 mM NaClO<sub>4</sub> aqueous solution.

In the **2**-poly(EDOT) film, the oxidized state showed a weak absorption band in the visible region and a strong absorption band in the near-IR region, whereas the reduced state showed a broad absorption band at 587 nm assigned to the  $\pi$ - $\pi^*$  electronic transition (Figure 3b). The cyclic voltammetry (CV) waves and the UV-visible spectral change were very similar to those reported for an EDOT/SDS (anionic micelle) system.<sup>[24]</sup> For the **1**-poly(EDOT) film, the oxidized state showed a broad absorption peak around 700 nm and a weak absorption band in the near-IR region, whereas the reduced state showed a broad absorption peak at 520 nm assigned to the  $\pi$ - $\pi^*$  electronic transition (Figure 3a). The absorption peaks in the **1**-poly(EDOT) film were shifted to a shorter wavelength than those in the **2**-poly(EDOT) film. This result indicates that poly(EDOT) obtained under basic conditions features a shorter conjugate length than that obtained under neutral pH conditions, which is attributed to the side reactions of EDOT with nucleophiles during the polymerization process.

To obtain concrete evidence that these films were composed of poly(EDOT) and lipid, attenuated total reflection (ATR) IR spectra of the modified ITO electrodes were measured. One can recognize new peaks (1571, 1675 (amide C=O), and 1735 cm<sup>-1</sup> (carboxylic acid C=O)) (shown by arrows in Figure 4a) for the **1**-poly(EDOT) composite film, which are not present in the film of poly(EDOT) obtained in the absence of **1** (dotted line). Similarly, a new peak appears at 1641 cm<sup>-1</sup> (amide C=O) (shown by an arrow, (Figure 4b)) in the **2**-poly(EDOT) composite film, which is not present in the film of poly(EDOT) obtained in the absence of **2**.

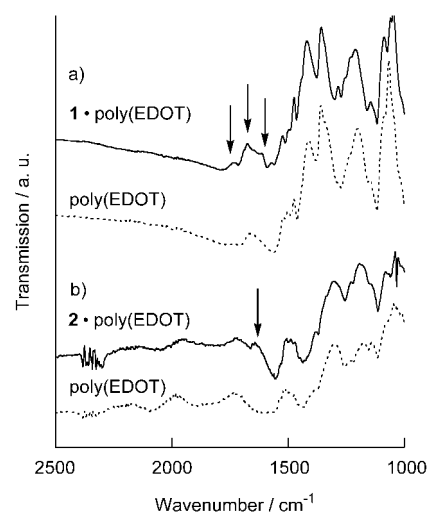


Figure 4. ATR IR spectra of electrochemically polymerized poly(EDOT) films; a) **1**-poly(EDOT) composite film (—) and poly(EDOT) film (---) obtained under basic conditions; b) **2**-poly(EDOT) composite film (—) and poly(EDOT) film (---) obtained under neutral pH conditions.

To obtain visual images of these composite films, we took SEM pictures (Figure 5). Electrochemical polymerization of EDOT in the presence of **1** (after 4 and 7 cycles) resulted in a right-handed helical structure (Figure 5a) whereas in the presence of **2** it resulted in a left-handed helical structure (Figure 5b). The helical motif of the resultant lipid-poly(EDOT) composites is in accordance with that of the lipid aggregates (see Figure 1) which are expected to act as the templates. It is also seen from these images that the size of the helical tapes increases with the increase in the number of redox cycles (Figure 5a). This implies that the incipient **1**-conjugate-polymer composites are successively adsorbed

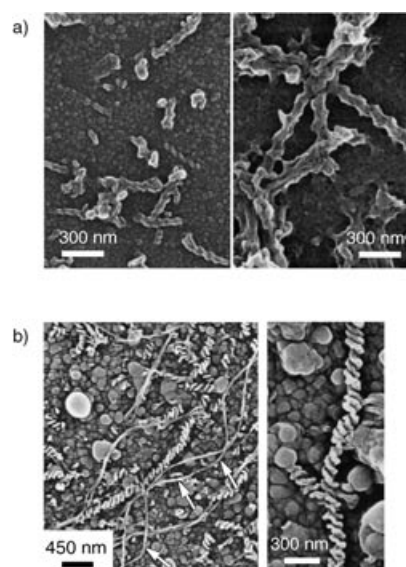


Figure 5. SEM images of electrochemically polymerized poly(EDOT) films; a) **1**-poly(EDOT) composite film obtained under basic conditions after 4 (left) and 7 (right) redox cycles; b) **2**-poly(EDOT) composite film obtained under neutral pH conditions after 60 redox cycles.

onto the ITO electrode surface and then grow up to become "fat" helical tapes on the surface. Here one must also consider that the poly(EDOT) film may be initially formed on the ITO electrode and the helical lipid aggregates may just be adsorbed onto the film surface. To exclude this possibility we conducted the following reference experiment. The poly(EDOT) films were prepared in the absence of the lipid molecule and then immersed in an aqueous solution containing each lipid molecule. The SEM pictures of the resultant modified ITO electrodes only showed pebble-like masses, similar to those observed in the background under the helical structure.

Figure 5b displays confirmation of the creation of left-handed helical aggregates composed of poly(EDOT) polymer bundles. The helical motif (pitch length = 50–70 nm) is in accordance with that of the template composed of the aggregate of synthetic lipid **2** (pitch length = 50–70 nm, estimated from Figure 1b). In addition, one can clearly recognize a unique superstructure consisting of two intertwined fibrils (shown by arrows). The creation of similar double-stranded structures was also reported for the silica nanofibers prepared by the sol-gel reaction of tetraethoxysilane using a gemini surfactant as a template<sup>[15]</sup> and poly(pyrrole) nanofibers prepared by chemical polymerization using a zwitterionic lipid aggregate as a template.<sup>[25]</sup> EDOT polymerization proceeds preferentially along the two edges of the sheet structure where the density of negative charges is higher and the molecules are more exposed to the solvent because of the sharp curvature.<sup>[25,26]</sup> It is reasonable to consider, therefore, that the intertwined fibrils are created using the huge sheet structure (Figure 1) as the template; so polymerization will proceed along the two edges of this sheet. In fact, the distance between two fibrils (100–200 nm) is comparable with the sheet width of the original organic template. To evaluate components of the fibrous structure, we conducted energy dispersive X-ray (EDX) analyses of the polymers formed in the electrochemical cell in the presence of **1** (Figure 6), without staining treatment. It is seen from Figure 6 that a network structure observed for the TEM image (Figure 6 left) precisely overlaps with both a nitrogen map (Figure 6 center) associated with **1** and a sulfur map (Figure 6 right) associated with EDOT.

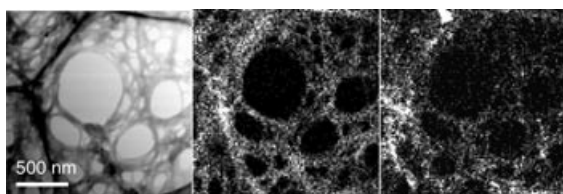


Figure 6. TEM image (left) and EDX pictures (center: nitrogen map, right: sulfur map) of a **1**-poly(EDOT) polymeric network created in the polymerization solution after electrochemical polymerization under basic conditions.

It occurred to us that electrochemical polymerization of pyrrole, the mechanism of which is basically similar to that of EDOT, would also proceed under the template effect. The poly(pyrrole) film is more rigid than the poly(EDOT) film and once formed, is scarcely soluble in any solvent; this

means that the morphology-controlled poly(pyrrole) synthesis is highly significant. The concentrations of reactants for the electrochemical polymerization of pyrrole were similar to those for the electrochemical polymerization of EDOT (see Experimental Section). Figure 7 shows SEM images of the resultant **1**-poly(pyrrole) and **2**-poly(pyrrole) films.

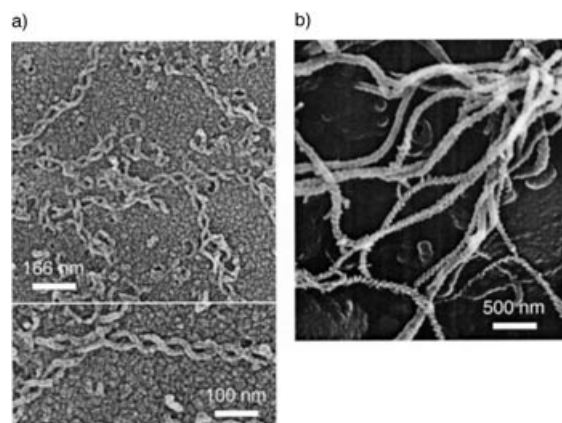


Figure 7. SEM images of a) **1**-poly(pyrrole) film electrochemically polymerized under basic conditions after 40 redox cycles and b) **2**-poly(pyrrole) film after 60 redox cycles under neutral pH conditions.

As shown in Figure 7a, one can clearly recognize that the bundle has a unique superstructure consisting of two intertwined fibrils, like those observed for the **2**-poly(EDOT) composite film (arrows in Figure 5b). Figure 7b shows that poly(pyrrole) obtained in the presence of **2** features the fibrous structure with left-handed helical motif, which is consistent with that observed for the **2**-poly(EDOT) composite film (see Figure 5b). These results indicate that templating electrochemical polymerization of pyrrole was also achieved by employing an anionic lipid aggregate as a template.

Poly(aniline) is also a kind of conjugate polymer. It can be easily produced in acidic solution and its conducting form is stable even in air or water. As an aniline monomer is protonated under the acidic polymerization conditions, one can expect that the electrostatic interaction between the propagating polymer and the anionic template will operate more efficiently than that between the EDOT or pyrrole polymer and the anionic template. We conducted the oxidative polymerization of aniline in the presence of **2** in an aqueous solution of H<sub>2</sub>SO<sub>4</sub> (50 mM) containing 10 vol % MeOH (see Experimental Section).<sup>[27]</sup> Electrochemical polymerization of aniline in the presence of **2** gave a redox-active poly(ANI) film on the ITO electrode (Figure 8).

In SEM studies of the obtained poly(ANI) film (Figure 9), one can recognize a left-handed helical superstructure similar to that observed for the **2**-poly(pyrrole) composite film (see Figure 7b). The density of the fibrous structure in this poly(ANI) film was higher than that in the poly(EDOT) and poly(pyrrole) films, indicating that the templating effect of protonated aniline is indeed more efficient than that of EDOT and pyrrole.

The preceding findings establish that as a general principle, the morphology of conjugate polymers is controllable,

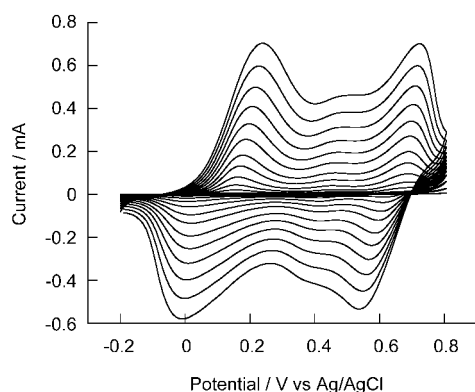


Figure 8. Cyclic voltammograms for aniline obtained on an ITO electrode in the presence of **2** in a 50 mM H<sub>2</sub>SO<sub>4</sub> aqueous solution containing 10 vol % MeOH.

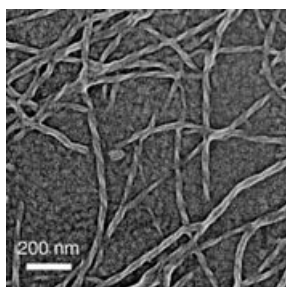


Figure 9. SEM images of the poly(ANI) composite film obtained from electrochemical polymerization in the presence of **2** after 100 redox cycles.

as in the case of the “templating sol–gel reaction” of cationic templates,<sup>[10–18]</sup> by employing anionic lipid aggregates as templates.

**Chemical polymerization of pyrrole, EDOT, and aniline by a templating method:** To obtain a mechanistic insight into the templating process, the TEM analysis of lipid-conjugate-polymer composites is very helpful. To prepare the TEM samples, however, one must peel the film off the ITO electrode surface, and the superstructure can be destroyed by this treatment. Thus, we prepared the lipid-conjugate-polymer composites by chemical polymerization of the corresponding monomer. Pyrrole, EDOT, and aniline can be chemically polymerized with ammonium peroxodisulfate (APS). Chemical polymerization of these monomers with APS was therefore carried out in the presence of **1** or **2**. The concentrations of reactants used for chemical polymerization were almost the same as those used for electrochemical polymerization (see Experimental Section). APS was added to the reaction solution to initiate the polymerization and the mixture was kept at 25 °C (see Experimental Section). The mixture was dialyzed (500 Da) to give lipid-poly(pyrrole) composites as black precipitates. These precipitates were subjected to TEM analysis without any staining treatment. One may consider, therefore, that the observed contrast is due to the formation of conjugate polymers.

Figure 10 shows the TEM images of the **1**-poly(pyrrole) composites. Since these TEM pictures were taken without

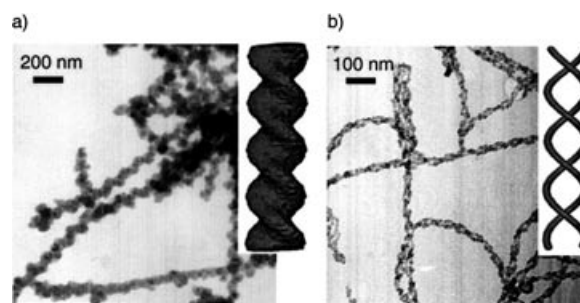


Figure 10. TEM images of **1**-poly(pyrrole) composites with a) large helical bundles, b) small double-strand-like helical fibers obtained from chemical polymerization. The TEM analysis was performed without staining treatment.

staining treatment, the shadows are attributed to poly(pyrrole) aggregates. One can recognize the coexistence of two different types of helical fibers, large helical bundles (Figure 10a) and double-strand-like, intertwined fibers (Figure 10b). It is known, from a few preceding transcription systems, that two different superstructures can be created from the same template;<sup>[15,19,28]</sup> that is, when the polymerization proceeds along the two edges of a helical-tape template followed by elimination of the template, the double-stranded superstructure is generated. In contrast, when the polymerization proceeds further, this tape template structure is completely covered by polymers resulting in the large helical bundles. In the present system, we presume that the fabrication starting in the early reaction stages yields the large helical bundles, whereas fabrication starting in the later reaction stages yields the small double-stranded fibers. An SEM image of **1**-poly(pyrrole) composites (Figure S1 in the Supporting Information) showed that the obtained precipitates consisted mostly of fibrous structures. This result clearly showed that the chemical polymerization method is better for obtaining the **1**-poly(pyrrole) composites with controlled morphology than the electrochemical polymerization method.

Figure 11 shows TEM images of **2**-poly(pyrrole) composites. As mentioned above, **2** provides two different aggregate morphologies useful for the templates, a left-handed fibrous structure and a huge sheet structure. As observed in Figure 10 for the **1**-templated system, the resultant polymeric morphologies are also affected by the reaction period. It

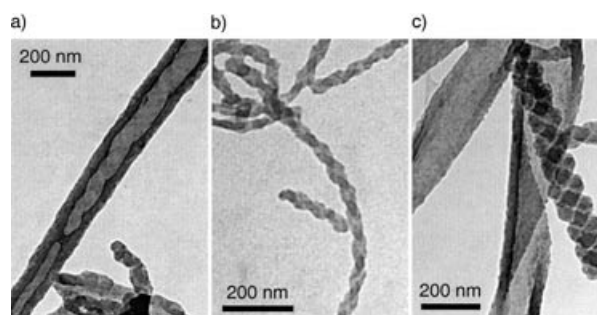


Figure 11. TEM images of **2**-poly(pyrrole) composites with a) a helical hollow structure and a large helical fiber and b) double-strand-like aggregates and a small structural size obtained from chemical polymerization. TEM analysis was performed without staining treatment.

can be expected, therefore, that four different polymeric aggregates may be formed from the **2**-templated system. One of these is a large tubular fiber with a hollow of approximately 100 nm (Figure 11a). Careful examination of the TEM image revealed that the helical structure of the template is engraved on the inside wall of the tubular fiber. As explained above, we presume that these large fibrous aggregates are formed by the fabrication starting in the early stages of the chemical polymerization using the left-hand fibrous structure as a template. In addition to these large fibrous aggregates, the smaller, double-strand-like aggregates are also formed (Figure 11b). These aggregates should be generated by the fabrication starting in the later stages of the chemical polymerization. In contrast, sheet-like polymeric aggregates are also observed (Figure 11c). It is undoubtable that this morphology is created by using the sheet-like structure as a template. As the polymeric structure should be fragile (compared with the fibrous structure), we consider that it is produced only by the fabrication starting in the early stage of the oxidative reaction.

TEM images of the **2**-poly(EDOT) composites prepared by chemical oxidation with APS are shown in Figure 12. As mentioned above, **2** aggregates into two different morpholo-

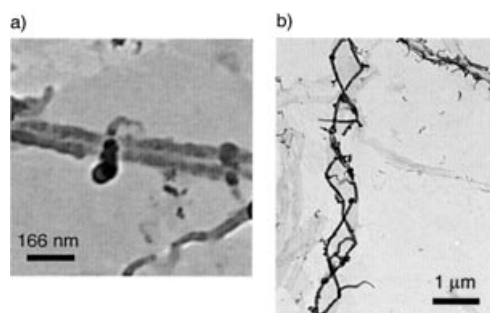


Figure 12. TEM images of the **2**-poly(EDOT) composites prepared by chemical polymerization. TEM analysis was performed without staining treatment.

gies. Complementary to the SEM pictures in Figure 5b, chemical polymerization of EDOT also resulted in two different superstructures. One is a tubular structure that is created by a template effect of the helical fiber (Figure 12a) and the other is a double-strand-like, intertwined duplex structure that is created by a template effect of the sheet (Figure 12b). The result in Figure 12b also shows that chemical polymerization of EDOT allows the propagation along the two edges of the sheet structure. The oxidative reactivity of EDOT is much inferior to that of pyrrole. Because of this difference in reactivity, neither a large hollow fiber nor a sheet-like structure (as observed in Figure 11a and Figure 11c, respectively, for poly(pyrrole)) was produced from EDOT.

Similarly, **2**-poly(ANI) composites obtained by chemical polymerization of aniline with APS also showed a tubular structure, the size of the hollow being comparable with that of the template aggregate (Figure 13).

These findings support the view, as a general concept, that the two edges of anionic helical aggregates act as a nucleus

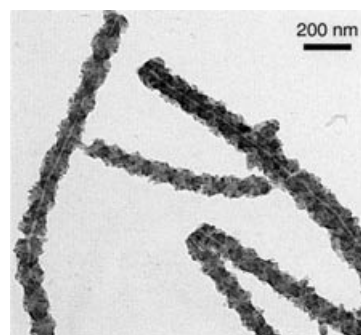


Figure 13. TEM images of **2**-poly(ANI) composites prepared from chemical polymerization with APS. TEM analysis was performed without staining treatment.

of the polymer growth and produce the transcribed polymer composites, the apparent morphology of which differs depending on conditions such as the reaction time and monomer concentration.

A slightly turbid solution of the **2**-poly(ANI) composite was subjected to circular dichroism (CD) analysis. As shown in Figure 14, a minimum in the CD signal was observed at

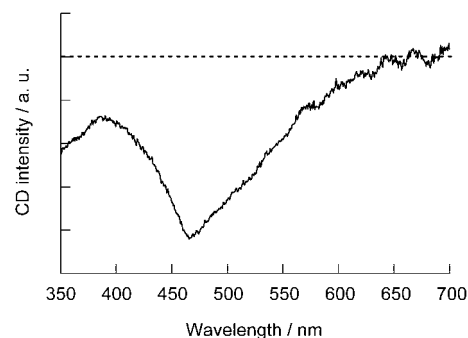


Figure 14. CD spectrum of the **2**-poly(ANI) composite dispersed in a 50 mm  $\text{H}_2\text{SO}_4$  aqueous solution. A weak linear dichroism (LD) peak appears at around 500 nm, the intensity of which is much weaker than the CD band at 465 nm.

465 nm, which is assigned to the absorbance of chiral poly(ANI).<sup>[2,29]</sup> The CD spectrum, together with TEM and SEM observations, indicates that the **2**-poly(ANI) composite has a factor of chirality even below the molecular level. Presumably, the multipoint interaction between protonated aniline and the chiral anionic template is strong enough to induce the chiral twisting in the **2**-poly(ANI) composite.

#### In situ conductivity measurements of **2**-poly(EDOT) and **2**-poly(ANI) films:

Pt-coated interdigitated microelectrodes were used for in situ conductivity measurements<sup>[30,31]</sup> of the **2**-poly(EDOT) and **2**-poly(ANI) composites. The polymers were produced by electrochemical polymerization under the same conditions as those for the ITO electrode. As shown in atomic force microscopy (AFM) images of **2**-poly(EDOT) composites electrochemically deposited on interdigitated microelectrodes (Figure 15a), the bridge between two electrodes is attained only by templated fibers composed of **2** and poly(EDOT). Figure 15a shows that nontemplating poly(EDOT) random structures are adsorbed onto the sur-

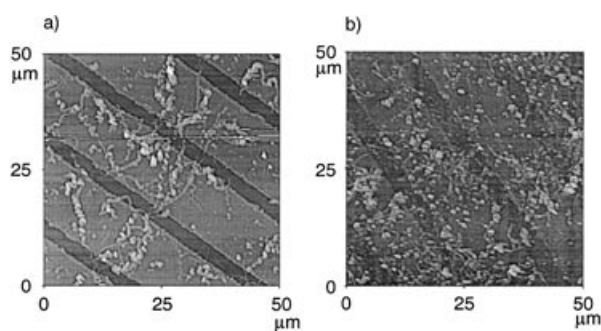


Figure 15. AFM images of electrochemical polymerized a) **2**-poly(EDOT) composites on interdigitated microelectrodes after 50 redox cycles and b) **2**-poly(ANI) composites on interdigitated microelectrodes after 40 redox cycles.

face of the microelectrodes and do not bridge the two electrodes. It is seen from Figure 15b that the bridge between the two electrodes is attained mostly by templated helical fibers composed of **2** and poly(ANI). In other words, poly(ANI) random structures generated without the template scarcely bridge the two electrodes.

The conductance measurements of the poly(EDOT) polymer were carried out in an aqueous solution of NaClO<sub>4</sub> (50 mM) and those for the poly(ANI) polymer were carried out in an aqueous solution of H<sub>2</sub>SO<sub>4</sub> (50 mM). The conductivity was estimated by holding one Pt line at a fixed potential, V<sub>g</sub>, versus Ag/AgCl and the other at V<sub>g</sub>+20 mV. The potential difference between the electrodes results in a current flow (drain current). In the poly(EDOT) film, the drain current was scarcely observed below −0.5 V, then increased above −0.5 V, and reached a plateau at +0.1 V (Figure 16a).<sup>[31]</sup> In the poly(ANI) film, the drain current was scarcely observed below 0 V, then increased above 0 V, and reached a plateau at +0.2 V (Figure 16b). These results are basically similar to those reported in reference [30] and indicate that the observed conductivity is due to the lipid-conjugate-polymer fibrous composites.

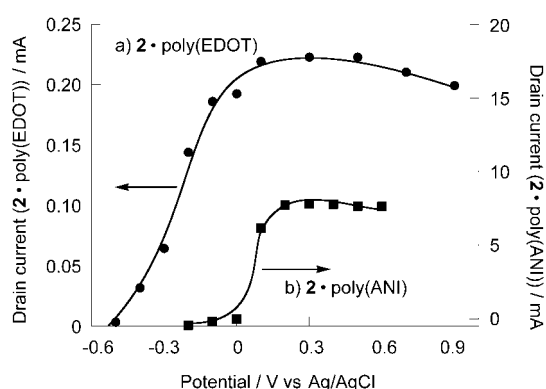
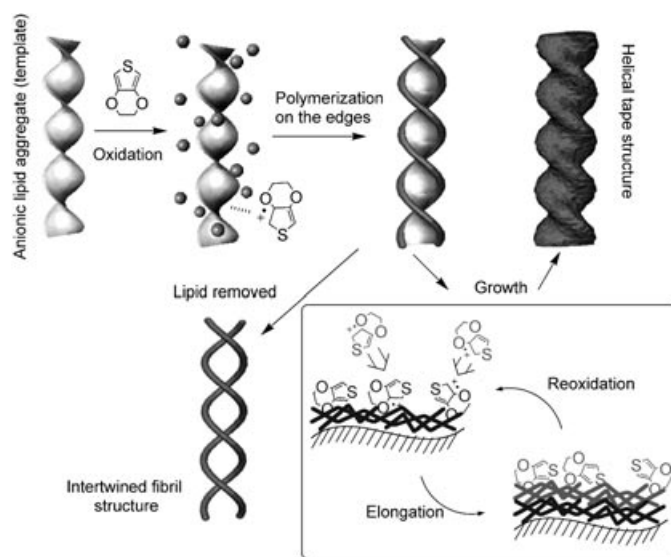


Figure 16. Drain current versus gate voltage (V<sub>g</sub>) plots for the a) **2**-poly(EDOT) composite and b) **2**-poly(ANI) composite.<sup>[32]</sup>

## Conclusion

In conclusion, the present study has demonstrated, for the first time to the best of our knowledge, that the morphology

of the poly(EDOT), poly(pyrrole), and poly(ANI) films obtained by electrochemical polymerization of EDOT, pyrrole, and aniline, respectively, can be controlled by using anionic, synthetic lipid assemblies as templates. This novel templating process is shown schematically in Scheme 2. As demon-



Scheme 2. Schematic illustration of a templating method for oxidative polymerization.

strated in the present study, this templating method is applicable to different lipid assemblies, different monomers, and different oxidation procedures. One may therefore regard the present templating method as a very general concept. Until now, it was believed that in the oxidative polymerization of these monomers the convenience of the preparative method was an advantage, whereas the difficulty in the morphology control was a serious disadvantage. This disadvantage, possibly bigger than the advantages so far, has hampered the broad application of these conjugate polymers as functional materials. Therefore, we now believe that as this problem has been solved (at least partially), the present study will stimulate further utilization of these polymers as new functional materials. We consider that in principle, the various polymeric superstructures can be created from poly(EDOT), poly(pyrrole), and poly(ANI) as long as the appropriate “anionic” assemblies suitable for the template exist.

## Experimental Section

The synthetic procedures for **1**<sup>[20]</sup> and **2**<sup>[21]</sup> were reported previously.

**General methods:** CV experiments were performed with a one-compartment, three-electrode electrochemical cell driven by an electrochemical analyzer (Autolab PGSTAT12 potentiostat/galvanostat or BAS 100B) in aqueous solution. Conductivity measurements were carried out using Autolab PGSTAT12 with BIPOT bipotentiostat. AFM studies were carried out on a Topometrix TMX-2100 (noncontact mode). SEM studies were carried out on a Hitachi S-5000. TEM and EDX studies were carried out on a FEI tecnai-20 or a JEOL JEM-2010. ATR IR spectra were recorded with a PerkinElmer Spectrum One.

**Materials:** Pyrrole (Tokyo Kasei Kogyo) was used after distillation. Ethylenedioxythiophene (Aldrich), aniline (Wako Chemicals), H<sub>2</sub>SO<sub>4</sub> (Kishida Chemicals) and sodium perchlorate (Tokyo Kasei Kogyo) were used as received.

**Preparation of 1-poly(EDOT) by electrochemical polymerization:** A solution of triethylene glycol (0.1 mL) containing EDOT (10 mg) was mixed with water (10 mL) under sonication. To this solution, **1** (2.0 mg), NaOH aqueous solution (1 M, 20  $\mu$ L), and LiCl (21 mg) were added. The final concentrations were [EDOT]=7.1 mM, [LiCl]=50 mM, [NaOH]=2.0 mM, and [**1**]=0.33 mM. The cell consisted of an ITO electrode as the working electrode (working area=2.2 cm<sup>2</sup>), a Pt counter electrode, and an Ag/AgCl reference electrode. The redox was repeated in a voltage range of 0.4–1.3 V (vs Ag/AgCl) with a scan rate of 0.05 V s<sup>-1</sup> at 25 °C. After electrochemical polymerization, 5 redox cycles were performed in the electrolyte solution in the absence of the lipid molecules to wash the electrode.

**Preparation of 2-poly(EDOT) by electrochemical polymerization:** Compound **2** (2.1 mg), EDOT (13 mg), and NaClO<sub>4</sub> (61 mg) were dissolved in 10 vol % MeOH aqueous solution (10 mL). The final concentrations were [EDOT]=9.4 mM, [NaClO<sub>4</sub>]=50 mM, and [**2**]=0.3 mM. The cell consisted of an ITO electrode as the working electrode (working area=2.2 cm<sup>2</sup>), a Pt counter electrode, and an Ag/AgCl reference electrode. The redox was repeated in a voltage range of -0.5–0.9 V (vs Ag/AgCl) with a scan rate of 0.05 V s<sup>-1</sup> at 25 °C. After electrochemical polymerization, 5 redox cycles were performed in the electrolyte solution in the absence of the lipid molecules to wash the electrode.

**Preparation of 2-poly(EDOT) by chemical polymerization:** Compound **2** (2.1 mg), EDOT (13 mg), and NaClO<sub>4</sub> (61 mg) were dissolved in 10 vol % MeOH aqueous solution (10 mL). The final concentrations were [EDOT]=9.4 mM, [NaClO<sub>4</sub>]=50 mM, and [**2**]=0.3 mM. APS (4 mg) was added to 1 mL of the solution. After 1 day at 25 °C, dialysis (500 Da) was performed for 1 day.

**Preparation of 1-poly(pyrrole) by electrochemical polymerization:** A solution of triethylene glycol (0.1 mL) containing pyrrole (10 mg) was mixed with water (10 mL) under sonication. To this solution, **1** (2.0 mg), NaOH aqueous solution (1 M, 20  $\mu$ L), and LiCl (21 mg) were added. The final concentrations were [pyrrole]=15 mM, [LiCl]=50 mM, [NaOH]=2.0 mM, and [**1**]=0.33 mM. The cell consisted of an ITO electrode as the working electrode (working area=2.2 cm<sup>2</sup>), a Pt counter electrode, and an Ag/AgCl reference electrode. The redox was repeated in a voltage range of 0.4–1.15 V (vs Ag/AgCl) with a scan rate of 0.05 V s<sup>-1</sup> at 25 °C. After electrochemical polymerization, 5 redox cycles were performed in the electrolyte solution in the absence of the lipid molecules to wash the electrode.

**Preparation of 1-poly(pyrrole) by chemical polymerization:** A solution of triethylene glycol (0.1 mL) containing pyrrole (10 mg) was mixed with water (10 mL) under sonication. To this solution, **1** (2.0 mg), NaOH aqueous solution (1 M, 20  $\mu$ L), and LiCl (21 mg) were added. APS (2.3 mg) was added to 1 mL of the solution. After 45 minutes at 25 °C, dialysis (500 Da) was performed for 1 day.

**Preparation of 2-poly(pyrrole) by electrochemical polymerization:** Compound **2** (2.1 mg), pyrrole (10  $\mu$ L), and NaClO<sub>4</sub> (61 mg) were dissolved in 10 vol % MeOH aqueous solution (10 mL). The final concentrations were [pyrrole]=14 mM, [NaClO<sub>4</sub>]=50 mM, and [**2**]=0.3 mM. The cell consisted of an ITO electrode as the working electrode (working area=2.2 cm<sup>2</sup>), a Pt counter electrode, and an Ag/AgCl reference electrode. The redox was repeated in a voltage range of -0.5–0.8 V (vs Ag/AgCl) with a scan rate of 0.05 V s<sup>-1</sup> at 25 °C. After electrochemical polymerization, 5 redox cycles were performed in the electrolyte solution in the absence of the lipid molecules to wash the electrode.

**Preparation of 2-poly(pyrrole) by chemical polymerization:** Compound **2** (2.1 mg), pyrrole (10  $\mu$ L), and NaClO<sub>4</sub> (61 mg) were dissolved in 10 vol % MeOH aqueous solution (10 mL). The final concentrations were [pyrrole]=14 mM, [NaClO<sub>4</sub>]=50 mM, and [**2**]=0.3 mM. APS (4.6 mg) was added to 1 mL of the solution. After 30 minutes at 25 °C, dialysis (500 Da) was performed for 1 day.

**Preparation of 2-poly(ANI) by electrochemical polymerization:** Compound **2** (2.1 mg) and aniline (71 mg) were dissolved in water (9 mL) containing MeOH (1 mL). To this solution, H<sub>2</sub>SO<sub>4</sub> (0.5 M, 1 mL) was added. The final concentrations were [aniline]=50 mM, [H<sub>2</sub>SO<sub>4</sub>]=50 mM,

and [**2**]=0.3 mM. The cell consisted of an ITO electrode as the working electrode (working area=2.2 cm<sup>2</sup>), a Pt counter electrode, and an Ag/AgCl reference electrode. The redox was repeated in a voltage range of -0.2–0.8 V (vs Ag/AgCl) with a scan rate of 0.05 V s<sup>-1</sup> at 25 °C. After electrochemical polymerization, 5 redox cycles were performed in the electrolyte solution in the absence of the lipid molecules to wash the electrode.

**Preparation of 2-poly(ANI) by chemical polymerization:** Compound **2** (2.1 mg) and aniline (71 mg) were dissolved in water (9 mL) containing MeOH (1 mL). To this solution, H<sub>2</sub>SO<sub>4</sub> (0.5 M, 1 mL) was added. The final concentrations were [aniline]=50 mM, [H<sub>2</sub>SO<sub>4</sub>]=50 mM, and [**2**]=0.3 mM. APS (22 mg) was added to 2 mL of the solution. After 30 minutes at 25 °C, dialysis (500 Da) was performed for 2 days.

## Acknowledgment

We thank Ms. Kitada for her helpful assistance with the AFM measurements.

- [1] a) K. Tajima, T. Aida, *Chem. Commun.* **2000**, 2399–2412; b) L. Brunsveld, B. J. B. Folmer, E. W. Meijer, R. P. Sijbesma, *Chem. Rev.* **2001**, *101*, 4071–4097; c) M. B. J. Otten, C. Ecker, G. A. Metselaar, A. E. Rowan, R. J. M. Nolte, P. Samor, J. P. Rabe, *ChemPhysChem* **2004**, *5*, 128–130.
- [2] a) D. T. McQuade, A. E. Pullen, T. M. Swager, *Chem. Rev.* **2000**, *100*, 2537–2574; b) A. Kros, R. J. M. Nolte, N. A. J. M. Sommerdijk, *Adv. Mater.* **2002**, *14*, 1779–1782.
- [3] a) J. Huang, S. Virji, B. H. Weiller, R. B. Kaner, *J. Am. Chem. Soc.* **2003**, *125*, 314–315; b) W. Li, H.-L. Wang, *J. Am. Chem. Soc.* **2004**, *126*, 2278–2279.
- [4] T. Iyoda, M. Ando, T. Kaneko, A. Ohtani, T. Shimizu, K. Honda, *Langmuir* **1987**, *3*, 1169–1170.
- [5] W. Wernet, M. Monkenbusch, G. Wegner, *Macromol. Rapid Commun.* **1984**, *5*, 157–164.
- [6] a) M. Kanungo, A. Kumar, A. Q. Contractor, *J. Electroanal. Chem.* **2002**, *528*, 46–56; b) Z. Zhong, M. Wan, *Synth. Met.* **2002**, *128*, 83–89; Z. Zhong, M. Wan, *Adv. Mater.* **2002**, *14*, 1314–1317; c) L. Qu, G. Shi, *Chem. Commun.* **2003**, 206–207; d) Z. Wei, M. Wan, T. Lin, L. Dai, *Adv. Mater.* **2003**, *15*, 136–139.
- [7] a) J. F. Hulvat, S. I. Stupp, *Angew. Chem.* **2003**, *115*, 802–805; *Angew. Chem. Int. Ed.* **2003**, *42*, 778–781.
- [8] J. H. Georger, A. Singh, R. R. Price, J. M. Schnur, P. Yager, P. E. Schoen, *J. Am. Chem. Soc.* **1987**, *109*, 6169–6175.
- [9] a) M. Ikegame, K. Tajima, T. Aida, *Angew. Chem.* **2003**, *115*, 2204–2207; *Angew. Chem. Int. Ed.* **2003**, *42*, 2154–2157; b) G. Li, S. Bho-sale, T. Wang, Y. Zhang, H. Zhu, J. H. Fuhrhop, *Angew. Chem.* **2003**, *115*, 3948–3951; *Angew. Chem. Int. Ed.* **2003**, *42*, 3818–3821.
- [10] a) J. H. Jung, Y. Ono, K. Hanabusa, S. Shinkai, *J. Am. Chem. Soc.* **2000**, *122*, 5008–5009; b) J. H. Jung, Y. Ono, K. Sakurai, M. Sano, S. Shinkai, *J. Int. Biomed. Inf. Data* **2000**, *122*, 8648–8653; c) Y. Ono, K. Nakashima, M. Sano, J. Hojo, S. Shinkai, *J. Mater. Chem.* **2001**, *11*, 2412–2419.
- [11] S. Kobayashi, N. Hamasaki, M. Suzuki, M. Kimura, H. Shirai, K. Hanabusa, *J. Am. Chem. Soc.* **2002**, *124*, 6550–6551, and references therein.
- [12] a) A. M. Seddon, H. M. Patel, S. L. Burkett, S. Mann, *Angew. Chem.* **2002**, *114*, 3114–3117; *Angew. Chem. Int. Ed.* **2002**, *41*, 2988–2991, and references therein.
- [13] K. Katagiri, R. Hamasaki, K. Ariga, J. Kikuchi, *J. Am. Chem. Soc.* **2002**, *124*, 7892–7893.
- [14] J. H. Jung, S. Shinkai, T. Shimizu, *Nano Lett.* **2002**, *2*, 17–20.
- [15] K. Sugiyasu, S. Tamaru, M. Takeuchi, D. Berthier, I. Huc, R. Oda, S. Shinkai, *Chem. Commun.* **2002**, 1212–1213.
- [16] For recent reviews see a) G. J. de A. A. Soler-Illia, C. Sanchez, B. Lebean, J. Patorin, *Chem. Rev.* **2002**, *102*, 4093–4138; b) K. J. C. van Bommel, A. Friggeri, S. Shinkai, *Angew. Chem.* **2003**, *115*, 1010–1030; *Angew. Chem. Int. Ed.* **2003**, *42*, 980–999.



- [17] a) Y. Ono, K. Nakashima, M. Sano, Y. Kanekiyo, K. Inoue, J. Hojo, S. Shinkai, *Chem. Commun.* **1998**, 1477–1478; b) J. H. Jung, Y. Ono, S. Shinkai, *Chem. Eur. J.* **2000**, *6*, 4552–4557.
- [18] The helical structure of CdS has also been created: E. D. Sone, E. R. Zubarev, S. I. Stupp, *Angew. Chem.* **2002**, *114*, 1781–1785; *Angew. Chem. Int. Ed.* **2002**, *41*, 1705–1709.
- [19] a) T. Hatano, M. Takeuchi, A. Ikeda, S. Shinkai, *Chem. Commun.* **2003**, 342–343; T. Hatano, M. Takeuchi, A. Ikeda, S. Shinkai, *Chem. Lett.* **2003**, 314–315; b) T. Hatano, M. Takeuchi, A. Ikeda, S. Shinkai, *Org. Lett.* **2003**, *5*, 1395–1398; c) A.-H. Bae, T. Hatano, M. Numata, M. Takeuchi, S. Shinkai, *Chem. Lett.* **2004**, *33*, 436–437; d) T. Hatano, A.-H. Bae, K. Sugiyasu, N. Fujita, M. Takeuchi, A. Ikeda, S. Shinkai, *Org. Biomol. Chem.* **2003**, *1*, 2343–2347; e) A.-H. Bae, T. Hatano, N. Nakashima, H. Murakami, S. Shinkai, *Org. Biomol. Chem.* **2004**, *2*, 1139–1144.
- [20] For compound **1** see: H. Hachisako, Y. Murata, H. Ihara, *J. Chem. Soc. Perkin Trans. 2* **1999**, 2569–2577. For the helical structure of lipid molecules see: N. Nakashima, S. Asakuma, T. Kunitake, *J. Am. Chem. Soc.* **1985**, *107*, 509–510.
- [21] T. Hatano, A.-H. Bae, M. Takeuchi, N. Fujita, K. Kaneko, H. Ihara, M. Takafuji, S. Shinkai, *Angew. Chem.* **2004**, *116*, 471–475; *Angew. Chem. Int. Ed.* **2004**, *43*, 465–469.
- [22] P. Novak, *Electrochim. Acta* **1992**, *37*, 1227–1230.
- [23] S. Ghosh, G. A. Bowmaker, R. P. Cooney, J. M. Seakins, *Synth. Met.* **1998**, *95*, 63–67.
- [24] N. Sakmeche, S. Aciyah, J. J. Aaron, M. Jouini, L. C. Lacroix, P. C. Lacaze, *Langmuir* **1999**, *15*, 2566–2574.
- [25] M. Goren, Z. Qi, R. B. Lennox, *Chem. Mater.* **2000**, *12*, 1222–1228.
- [26] Y. M. Lcoc, R. R. Price, J. V. Selinger, A. Singh, M. S. Spector, J. M. Schnur, *Langmuir* **2000**, *16*, 5932–5935.
- [27] As compound **1** does not dissolve in acidic solution, polymerization of aniline in the presence of **1** cannot be performed.
- [28] S. Kawano, S. Tamaru, N. Fujita, S. Shinkai, *Chem. Eur. J.* **2004**, *10*, 343–351.
- [29] A. G. MacDiarmid, I. D. Norris, G. G. Wallace, W. Zheng, *Synth. Met.* **1999**, *106*, 171–176.
- [30] G. Schiavon, S. Sitran, G. Zotti, *Synth. Met.* **1989**, *32*, 209–217.
- [31] a) K. Krishnamoorthy, A. V. Ambade, S. P. Mishra, M. Kanungo, A. Q. Contractor, A. Kumar, *Polymer* **2002**, *43*, 6465–6470; b) M. Lapkowski, A. Pron, *Synth. Met.* **2000**, *110*, 79–83; c) M. C. Morvant, J. R. Reynolds, *Synth. Met.* **1998**, *92*, 57–61.
- [32] Because the interdigitated microelectrode gaps were not filled with helical fibers, it was difficult to convert the observed drain current to conductance.

Received: April 5, 2004

Published online: September 2, 2004